

Article

Modeling the Projected Changes of River Flow in Central Vietnam under Different Climate Change Scenarios

Tuan B. Le and Hatim O. Sharif *

Department of Civil and Environmental Engineering, University of Texas at San Antonio,
One UTSA Circle, San Antonio, TX 78249, USA; E-Mail: lebaotuan@gmail.com

* Author to whom correspondence should be addressed; E-Mail: hatim.sharif@utsa.edu;
Tel.: +86-210-458-6478; Fax: +86-210-458-6476.

Academic Editor: Miklas Scholz

Received: 25 May 2015 / Accepted: 1 July 2015 / Published: 7 July 2015

Abstract: Recent studies by the United Nations Environment Programme (UNEP) and the Intergovernmental Panel on Climate Change (IPCC) indicate that Vietnam is one of the countries most affected by climate change. The variability of climate in this region, characterized by large fluctuations in precipitation and temperature, has caused significant changes in surface water resources. This study aims to project the impact of climate change on the seasonal availability of surface water of the Huong River in Central Vietnam in the twenty-first century through hydrologic simulations driven by climate model projections. To calibrate and validate the hydrologic model, the model was forced by the rain gage-based gridded Asian Precipitation–Highly Resolved Observational Data Integration Towards Evaluation of water resources (APHRODITE) V1003R1 Monsoon Asia precipitation data along with observed temperature, humidity, wind speed, and solar radiation data from local weather stations. The simulated discharge was compared to observations for the period from 1951 until present. Three Global Climate Models (GCMs) ECHAM5-OM, HadCM3 and GFDL-CM2.1 integrated into Long Ashton Research Station-Weather Generator (LARS-WG) stochastic weather generator were run for three IPCC–Special Report on Emissions Scenarios (IPCC-SRES) emissions scenarios A1B, A2, and B1 to simulate future climate conditions. The hydrologic model simulated the Huong River discharge for each IPCC-SRES scenario. Simulation results under the three GCMs generally indicate an increase in summer and fall river discharge during the twenty-first century in A2 and B1 scenarios. For A1B scenario, HadCM3 and GFDL-CM2.1 models project a decrease in river discharge from present to the 2051–2080 period and then increase until the 2071–2100

period while ECHAM5-OM model produces opposite projection that discharge will increase until the 2051–2080 period and then decrease for the rest of the century. Water management impacts, such as irrigation or dam regulation, were not considered in this study. However, the results provide local policy makers with quantitative data to consider possible adjustment of future dam capacities for development of flood control policies.

Keywords: Asian Precipitation–Highly Resolved Observational Data Integration Towards Evaluation of water resources (APHRODITE); climate change; Global Climate Models (GCMs); Long Ashton Research Station-Weather Generator(LARS-WG); hydrologic modeling; Soil and Water Assessment Tool (SWAT); Huong River; flood control

1. Introduction

Numerous studies have shown that climate change significantly affects the hydrologic cycle and alters runoff regimes and water availability in different regions across the Globe [1–5]. In its fifth assessment report [6], the Intergovernmental Panel on Climate Change (IPCC) affirms that human development activities have caused large increases in greenhouse gases concentration in the atmosphere since 1850, mostly from burning fossil fuels and deforestation. These elevated concentrations cause temperature to rise on a global scale. The global increases in temperature appear to directly and significantly alter the hydrologic cycle through changing evapotranspiration (ET) and accumulation and melting of snow and ice [6]. In addition, climate change, as indicated by changes of atmospheric circulation, also significantly modifies precipitation patterns, intensities, and amounts at global scales [7,8]. It could consequently disturb the balance of temporal and spatial distribution of water resources and cause large scale floods or long-term droughts. At the regional scale, climate change causes changes in discharge of rivers and streams that potentially reduce or increase the needed water availability for human activities [9,10].

Future climate changes associated with specific emission scenarios can be projected using Global Climate Models (GCMs). GCMs' output data can be used regionally, after disaggregation, to force hydrological models to simulate projected runoff and river discharge. An approach that is broadly used in many previous studies is to generate a baseline simulation based on observed meteorological data in the past and use the baseline meteorological data to force a hydrologic model to generate baseline hydrologic conditions [3,4,8,11–14]. The evaluation of future changes in river discharge is based on the comparison of projected results with the baseline and their differences. This method may eliminate or substantially reduce the internal bias or error of the models. A study by Wu *et al.* [14] indicated that projected climate change will have great impacts on snow dominant streams, leading to lower summer streamflows and warmer summer stream temperature with smaller effects on transient and rain dominant regimes in the northwestern region of the United States. Hamlet [15] studied the projected impacts of climate change on seasonal rainfall in the Pacific Northwest region of North America and performed hydrologic simulations to support water resources management, flood control, hydropower development and other water related environmental services in the region. Thodsen [16] combined climate model generated precipitation and potential evapotranspiration and a hydrologic model to study the impact of

climate change on six major Danish catchments and reported potential future increases in the 100-year and 1000-year precipitation leading to increases in discharge that are approximately twice as much.

River discharge in central Vietnam is highly fluctuating. A report of the Institute of Strategy and Policy On Natural Resources and Environment of Vietnam (ISPONRE) supported by the United Nations Environment Programme (UNEP) identified Vietnam as one of the most adversely effected countries by climate change during the last 50 years [17]. Recent studies on future global water availability and major continental rivers' future discharges also projected considerable increases in runoff in South East Asia region, and Vietnam in particular, in the twenty-first century [13,18,19]. Such projected increases in runoff vary from 10%–20% to 40%–50% among different studies depending on which GCMs and emission scenarios were selected for simulation. Weiland *et al.* [13] and Nohara *et al.* [19] analyzed seasonal water availability in Vietnam and neighboring countries and both studies reported that peak river discharges typically occurred in the summer and fall with river discharges significantly lower in the winter and spring. In the twenty-first century, Nohara *et al.* [19] projected an increase in discharge mostly in the summer and fall for the period from 2006 to 2100 and Weiland *et al.* [13] confirmed these conclusions. However, the projection of river discharge from these studies is limited for only IPCC Special Report on Emissions Scenarios (IPCC-SRES) scenario A1B and was not based on hydrologic modeling.

The rainy season in Central Vietnam spans the summer and fall which are characterized by heavy precipitation and flood events [20]. The region has minimal precipitation from December to April and precipitation increases significantly from May to November with high intensity and density precipitation events in July and August. Seasonal precipitation, especially in the summer and fall, has increased in the second half of the twentieth century and grown more obviously in the beginning of the twenty-first century [21]. This most likely has increased runoff and annual discharges of rivers in the region; however, it has not been analyzed and demonstrated in any previous study.

On the other hand, flood control policy of the local governments requires quantitative evaluation of river flow changes in the past as well as in the future. In fact, water resources related policies and laws have been recently established by the government of Vietnam as well as local governments in response to water resources degradation and negative impacts of global climate change on water resources. One of the latest decisions approved by the Prime Minister of Vietnam in September, 2013 regarding the national strategy for sustainably exploitation and usage of natural resources until 2020 with the vision to 2030 states that it is necessary to practice water saving nationwide and focus on solving the water shortage problem during the dry season in the major river basins [22]. Due to the fact that water resources are unevenly distributed both spatially and temporally, especially in central Vietnam where precipitation could range from 400 to 4000 mm/year among different places and about 70%–85% annual total water budget occur in the rainy season [23], it is suggested that reservoirs and dams be efficiently operated to store water in the rainy months and supply in the dry months. Dam and reservoir development is also an option due to the fact that Vietnam is facing seasonal water shortage and cannot ensure water safety (at the standard of 4000 m³/person/year) because about 63% of the national water budget comes from outside the country and might not be used for domestic supply [23].

The Huong River basin itself had three major dam projects built on its three main tributaries: Binh Dien dam on the Bo tributary, Huong Dien dam on the Huu Trach tributary and Ta Trach dam on the Ta Trach tributary. These dams are currently playing an important role in flood control besides generating hydro-power for the area. Both Binh Dien dam and Huong Dien dam are currently operating

at their maximum flood control capacities, 180 million m³ and 400 million m³ respectively; while Ta Trach dam is designed with about 400 million m³ capacity for flood control purposes [24,25]. Flood control within the Huong River basin could be improved to reduce the damage caused by floods if flow is forecasted ahead of time. Ngo & Nguyen [24] suggested that doubling the flood control capacities of Binh Dien and Huong Dien dam would reduce the inundation time with water level above three meters downstream of the Huong River during an extreme flood event to only three hours, instead of several days under the current capacities. In many years before 2010 when the hydroelectric dams had not been built, the Huong River's water was under serious salinization far from the coast into mainland reaches [26].

With all the issues mentioned above, this study aims to answer three major questions: How has river discharge in Central Vietnam changed in the past 60 years? How will seasonal total discharges vary in the 21st century because of climate change under the consideration of different IPCC-SRES scenarios? And what are the differences among projections produced by different GCMs? The study is focused on one mid-size river basin, the Huong River basin. Future climate data used in this study are based on three IPCC-SRES scenarios: A2, A1B and B1 [27]. The choice of the GCMs that simulate the scenarios strongly affects the projected changes of meteorological parameters [2]. In this study, three GCMs including ECHAM5-OM (Germany), HadCM3 (UK) and GFDL-CM2.1 (USA) are selected to simulate future daily meteorological data which serve as input to the hydrological model SWAT. River discharge simulations of SWAT are performed separately for each input dataset produced by a pair of GCM and IPCC-SRES. This will create nine different projections of river discharge.

2. Data and Methods

2.1. Study Area and Hydrologic Model

The study area in this paper is the Huong River basin that is located in Thua Thien Hue province in Central Vietnam. The basin has a drainage area of 2830 km² with three major tributaries that originate in the southern and western mountainous areas: the Ta Trach and Huu Trach tributaries, which unite and form the main stem of the Huong River, and the Bo tributary, which merges into the Huong River downstream (Figure 1). This basin is also the study area of Le *et al.* [28] and its topographic and meteorological characteristics are fully described therein.

Similarly to Le *et al.* [28], the Soil and Water Assessment Tool (SWAT) hydrologic model was used in this study with only discharge simulation components were applied. Le *et al.* [28] also provides description on how discharge is simulated in SWAT.

2.2. Historical Meteorological Data

Daily precipitation observations for the period from 1951 to 2007 were extracted from APHRODITE gage-based precipitation data at a spatial resolution of 0.25° × 0.25° while for the period from 2008 to 2012, the daily precipitation values were collected from local rain gages within the basin. The centers of the eight 0.25° × 0.25° grids of APHRODITE are shown in Figure 1. Precipitation data are re-grouped into seasonal precipitation; spring (March through May), summer (June through August), fall (September through November) and winter (December through February). Temperature, humidity, and wind speed

data were obtained for the period from 1951 to 2012 from the National Climatic Data Center (NCDC) of the US National Oceanic and Atmospheric Administration (NOAA) for station in Hue city (Figure 1). The satellite-based solar radiation data were obtained from the Atmospheric Science Data Center of the US National Aeronautics and Space Administration (NASA). These daily data have low spatial resolution of $1^\circ \times 1^\circ$. For that reason, the study area falls into only one cell whose boundaries are 17° N, 16° S, 107° W and 108° E. The location of the center of this grid is shown as the Solar Gage in Figure 1.

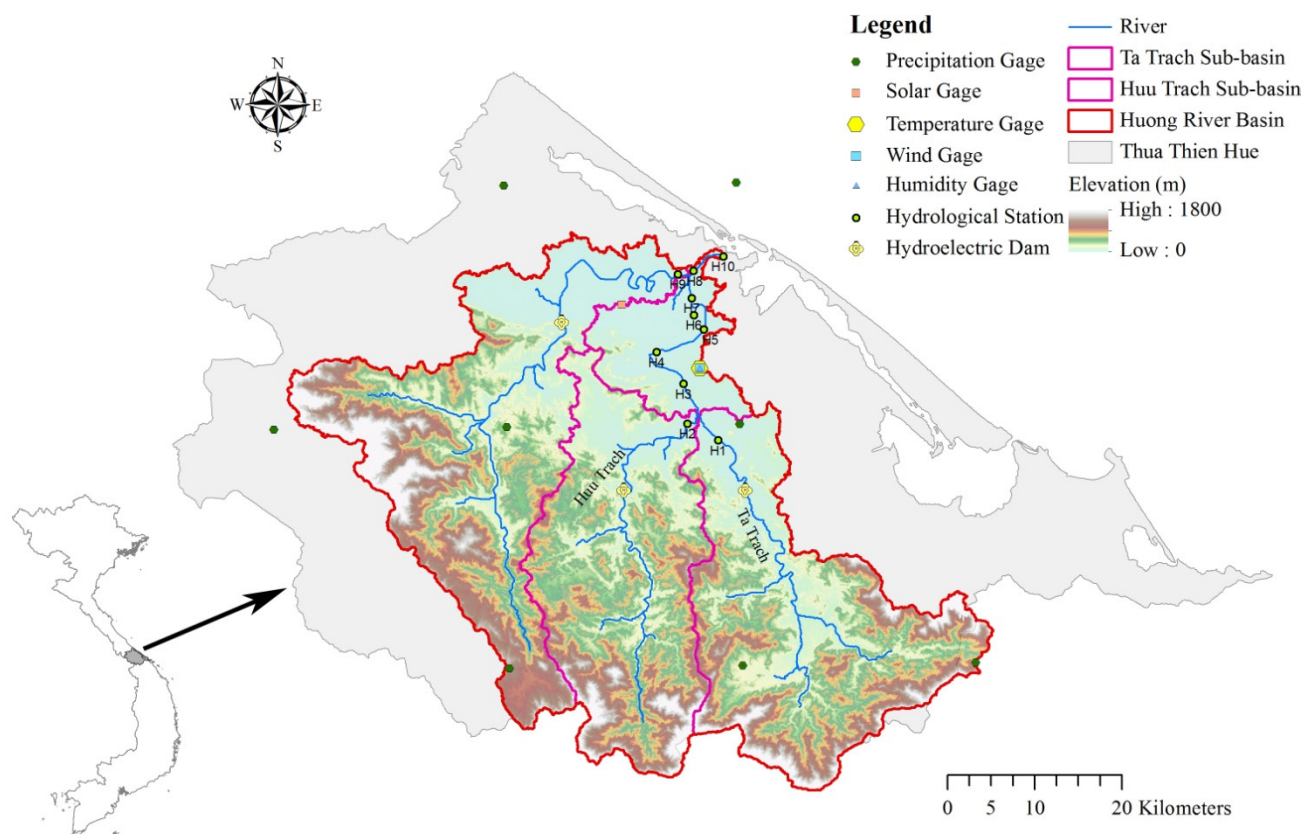


Figure 1. The Huong River basin in Central Vietnam [28]. Following SWAT model description of input data, what is described as “Gage” in the figure is actually the center of a grid for gridded data.

2.3. Modeled Future Climatic Changes

Projections from three GMCs included in the IPCC Fourth Assessment Report [27] are used in this study. Future climate simulations by each model were based on three future IPCC-SRES emission scenarios: A2 (high emission), A1B (medium emission) and B1 (low emission). The Long Ashton Research Station Weather Generator (LARS-WG) stochastic weather generator model was used to disaggregate GCM model output.

Observed daily meteorological data for a site are required to generate the probability distributions of each meteorological variable and their correlations by using semi-empirical distribution [29]. The simulation of precipitation in LARS-WG is based on alternating wet (nonzero precipitation) and dry periods with the length of each period being chosen arbitrarily from the appropriate distributions for a given month. On a wet day, the precipitation magnitude is estimated by using the semi-empirical

distribution of the precipitation for the month regardless of precipitation value of the previous days [30]. Daily maximum and minimum temperature are generated by using their statistical distributions and correlation with wet and dry conditions [31]. In general, daily temperature is lower for a wet day than a dry one. Similarly, solar radiation is generated using its semi-empirical distribution for wet and dry periods separately [30]. Details on the weather generation by LARS-WG were described by Racsco *et al.* [31], Semenov & Stratonovitch [29] and Semenov *et al.* [30]. LARS-WG version 5.5 was downloaded from the LARS-WG website [32].

There are three meteorological variables projected by the GCMs, precipitation, temperature and solar radiation. GCMs' outputs were disaggregated by LARS-WG into daily meteorological data at single sites (grid centers) based on the statistical properties of observation. Observed daily precipitation data from 1951 to 2012 were used to compute the probability distribution of wet and dry series as well as other LARS-WG parameters. Maximum and minimum daily temperature and solar radiation data were similarly used to generate probability distributions for the same period. The model then generated future meteorological data from 2013 to 2100 for precipitation, temperature, and solar radiation for each site based on statistics of historical data and future climate scenarios. Eight time series for eight precipitation gages (grid centers) were stochastically generated by LARS-WG. The ECHAM5-OM, HadCM3 and GFDL-CM2.1 models were used to simulate future climate conditions based on A2, A1B, and B1 scenarios. The A2 scenario describes a heterogeneous world with continuous increase in population and regionally oriented economic development that produce high emission of greenhouse gases and aerosols. The A1B scenario describes a rapid economic growth world with global population increases in the first half of the twenty-first century and declines in the second half of the century. The A1B scenario assumes a balance on fossil and non-fossil energy consumption of the world that produces medium emission of greenhouse gases and aerosols. The B1 scenario describes a world with social and environmental sustainability; greenhouse gases and aerosols emission is very low in this scenario [27]. These GCMs are widely used models that are regularly updated and improved by comparing their results against observed data [33].

2.4. Observed River Discharge Data

The Institute of Resources, Environment, and Biotechnology of Hue University, Vietnam (IREB-Hue) perform field measurements of flow discharge of the Huong River and its tributaries on a monthly basis. Measurements are taken on an arbitrary day of the month depending on weather conditions and the availability of employees. These discharge measurements are only available from 2007 to 2010. There are 10 measurement locations in the basin: three at the outlets of each tributary of Huong River (site H1, H2 and H9), six along Huong River from the confluence of Ta Trach River and Huu Trach River to the confluence of Huong River and Bo River (site H3, H4, H5, H6, H7 and H8), and one at the outlet of Huong River (site H10) before it pours into the lagoon (Figure 1). These monthly data are available in the annual reports of IREB-Hue.

Discharge measurements of the Huong River and its tributaries are calculated from measured flow velocities by multiplying them with the equivalent cross-sectional surface areas. Flow velocities are measured manually at the depth of 1.5 m below the water surface at specific locations across the channel. The equipment used to measure flow velocities is the Global Digital Water Flow Probe [34]. At each

channel cross-section, there are five to seven flow velocity measurements depending on the width of the river and the values are then averaged for that cross-section. Cross-sectional geometries and areas are constructed and calculated based on multiple depth measurements between the two riversides. These depth measurements of the riverbed are conducted by a Cole-Parmer Portable Water Depth Sounder Gage [34]. The measured discharges at the outlets of Ta Trach and Huu Trach tributaries as well as at the outlet of Huong River are used for calibration and validation of the SWAT model.

2.5. Projected Future Changes in River Discharge

Daily meteorological data including precipitation, maximum and minimum air temperature, and solar radiation at eight locations that correspond to the centers of the eight precipitation grids (Figure 1) are generated for the baseline period as well as for 2011–2100 periods by three GCMs ECHAM5-OM, HadCM3 and GFDL-CM2.1 for the three IPCC-SRES scenarios A2, A1B and B1. The simulated outputs include one dataset for the baseline and nine datasets for the future which are corresponding to nine pairs of GCM and emission scenario selected. These daily datasets then serve as meteorological input data for the calibrated SWAT model to simulate the Huong River discharge of corresponding periods. Average seasonal values were also calculated to identify the impact of climate change on seasonal discharge of the Huong River.

Outputs from the GCMs, disaggregated by LARS-WG to generate input to SWAT, were used to estimate projected river discharge. The average total seasonal discharge of each 30 year period was calculated and compared to the baseline discharge to see whether there are any significant changes in river discharge induced by projected climate change. The baseline used in this study is the 1961–1990 period. Climate data for the other 30-year periods: the 1951–1980, 1971–2000, 1981–2010 and 1991–2020 periods were also calculated. Projected values for the rest of the 21st century were calculated for the 2011–2040, 2021–2050, 2031–2060, 2041–2070, 2051–2080, 2061–2090 and 2071–2100 periods. The 30 year period used in this analysis is appropriate to represent the impact of climate change in the central decade due to the fact that the variability of water availability within a decade is not only impacted by climate change within that decade, but also the decade before [12].

The analysis of projected changes in the Huong River discharge includes the biases of the climate models that are contained in the models' outputs. Since climate models' biases do not only exist in the projected data; but also in the baseline; the comparison of projected future discharge to the baseline is still meaningful in evaluating the impact of climate change on changing the river discharge. In other words; the analysis of projected changes in the Huong River discharge is based on an assumption that climate models' biases are systematic and comparable in all models' outputs.

3. Results and Discussion

3.1. Calibration and Validation of River Discharge Simulations

SWAT calibration was performed over the catchment of Ta Trach tributary (site H1) for the period of 2007–2010, where the hydroelectric dam has no impact. The calibrated model parameters for the Ta Trach sub-basin were used to validate the model over the Huu Trach sub-basin at site H2 and the

Huong River basin at site H10 (Figure 1). The processes for SWAT model setup, simulation, calibration and validation for this region are described in detail in Le *et al.* [28].

The ArcSWAT for ArcGIS 10 interface of SWAT 2009 is used in this study to set up the model. Calibration was performed manually with ArcSWAT by adjusting the value of one model parameter at a time to attain better agreement between simulated and observed values. Veith *et al.* [35] reported that CH_N2 (Manning's N value for stream channels), CN2 (SCS curve number), SOL_K (soil hydraulic conductivity) and SOL_AWC (available water capacity of the soil) were the most significant SWAT model parameters that affect discharge simulation outputs. They also noted that the effects of ALPHA_BF (base flow alpha factor), ESCO (soil evaporation compensation factor) and GW_REVAP (groundwater "revap" coefficient) on model simulation could be considerable.

The model performance was evaluated through two standard performance measures: the Nash-Sutcliffe Efficiency (NSE) and the Pearson product-moment correlation coefficient (r). The NSE describes the predictive capability of the model and takes values that are smaller than or equal to one. Larger values of NSE that are closer to one indicate the model's ability to reproduce observed data. Pearson's r is a popular statistical measure that is used here to evaluate the degree of linear correlation between the simulated and observed variable. These measures are defined as follow:

$$NSE = 1 - \frac{\sum_{t=1}^N (Qo(t) - Qs(t))^2}{\sum_{t=1}^N (Qo(t) - \overline{Qo})^2} \quad (1)$$

$$r = \frac{\sum_{t=1}^N (Qs(t) - \overline{Qs})(Qo(t) - \overline{Qo})}{\sqrt{\sum_{t=1}^N (Qs(t) - \overline{Qs})^2 \sum_{t=1}^N (Qo(t) - \overline{Qo})^2}} \quad (2)$$

where $Qo(t)$ and $Qs(t)$ are the observed and simulated discharge at day t , respectively. \overline{Qo} and \overline{Qs} are the average observed and simulated discharge, respectively. N is the total number of observation/simulation days.

The discharge calibration process started with the adjustment of CH_N2 parameter. The NSE and r were calculated for every simulation and the value of adjusted model parameter that generated higher NSE and r than previous simulation was saved. The calibration process is continued by adjusting CN2, SOL_K, SOL_AWC, ALPHA_BF, ESCO and GW_REVAP, respectively, following the same procedure. The calibration process demonstrated that Huong River discharge was most sensitive to CH_N2 (Manning's N value for stream channels), CN2 (SCS curve number), and SOL_K (soil hydraulic conductivity). It was moderately sensitive to SOL_AWC (available water capacity of the soil) and ALPHA_BF (base flow alpha factor) and has low sensitivity to changes in ESCO (soil evaporation compensation factor) and GW_REVAP (groundwater "revap" coefficient).

Table 1 lists the values of the calibrated model parameters for discharge simulations. The values represent the calibrated parameters of the Huong River basin such as channel roughness, and hydraulic conductivity of soils that fall within their acceptable ranges in previous SWAT studies. The SCS curve number (CN) values, which are a function of land use, soil permeability, and antecedent soil moisture range between a lowest value of 42 to a highest of 97. The lower CN values are associated with the areas where forests dominate and sandy soils while the higher CN values apply to urban areas and wetlands. The hydraulic conductivity of each soil group slightly changed from their initial values after calibration. Dystric Gleysols at wetland areas had the lowest calibrated hydraulic conductivity of 0.318 mm/h,

Luvic Arenosols with mostly sand at the coastal areas had the highest calibrated hydraulic conductivity of 690.0 mm/h.

Table 1. Model parameters used to calibrate discharge at H1.

| Calibrated Model Parameters | | Calibrated Values |
|-----------------------------|--|-------------------|
| Parameters | Definitions (Unit) | |
| CH_N2 | Manning's N value for stream channels | 0.035 |
| CN2 | SCS curve number | 42–97 |
| SOL_K | Soil hydraulic conductivity (mm/h) | 0.318–690.0 |
| SOL_AWC | Available water capacity of the soil (mm/mm) | 0.075–0.315 |
| ALPHA_BF | Base flow alpha factor (days) | 0.25 |
| GW_REVAP | Groundwater “revap” coefficient | 0.02 |
| ESCO | Soil evaporation compensation factor | 1.0 |

The calibrated discharge of the Ta Trach sub-basin (H1) for the 2007–2010 period is shown in Figure 2. Due to the frequency of observed discharge, the comparison of simulated and observed discharge had to be performed at a daily time scale but with just one observed value for each month. The discharge hydrographs are shown in logarithmic scale because of the large differences between high and low flows (more than two orders of magnitudes). As can be seen from Figure 2, simulated discharge follows the fluctuations of observed discharge. The base flows during the dry seasons are relatively well simulated. However, the peak flows in the rainy seasons of 2007 and 2008 are slightly underestimated while overestimated in 2009 and 2010. Comparison of simulated and observed data points results in a Nash-Sutcliffe efficiency of 0.88 and a Pearson correlation coefficient of 0.94 (Table 2). In fact, errors in rainfall input and discharge measurement affect discharge simulation and calibration. APHRODITE rainfall products suffer from its very coarse resolution and cannot adequately capture the spatial and temporal distributions of extreme rainfall events. Discharge measurements were performed manually from a boat and have high potential of errors and bias. Nonetheless, the results are satisfactory based on model evaluation guidelines as well as compared to published SWAT simulations of daily discharge [36–38]. The calibration results were also improved compared to the previous study Le *et al.* [28] despite the same model parameters being used during calibration. This improvement is caused by the usage of input precipitation products. The higher accuracy of precipitation estimates brought by rain gage-based APHRODITE products than satellite-based TRMM products [39] used in Le *et al.* [28] contributed to better Nash-Sutcliffe efficiency and Pearson correlation coefficient of discharge calibration.

SWAT was validated over the Huu Trach sub-basin (H2) and the Huong River basin (H10). Discharge simulation at H2 (Figure 3) during the rainy season of 2007 has the same problem of underestimation observed at H1. Examining the APHRODITE precipitation for this period shows that it agrees with the simulated discharge pattern and does not match discharge observations. This indicates that the apparent underestimation is most probably a result of errors in either precipitation estimates or observed flow and is not caused by SWAT model errors. In general, observed discharges of the Huu Trach sub-basin (H2) and Huong River (H10) basin are reasonably estimated by SWAT. The fluctuations of simulated discharge match observed ones except for the deviation in 2007 rainy season at H2 (Figures 3 and 4). Simulated and observed discharge comparisons at H2 and H10 from January 2007 to December 2009

have Nash-Sutcliffe efficiencies of 0.72 and 0.73 and Pearson correlation coefficients of 0.85 and 0.91, respectively (Table 2).

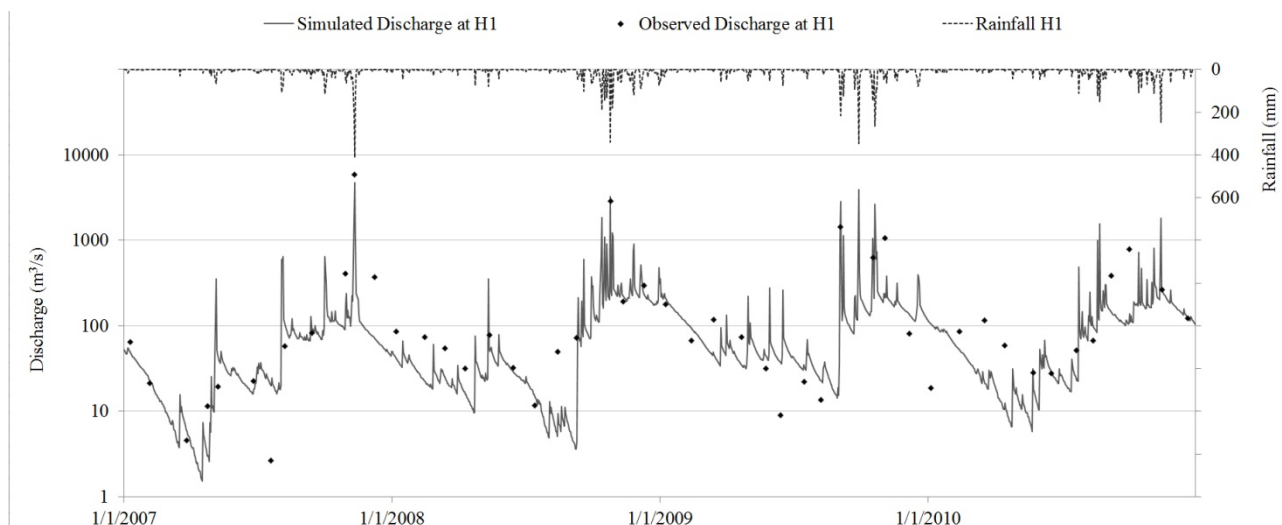


Figure 2. Discharge calibration at H1.

Table 2. Performance evaluation statistics of discharge simulation.

| Station | Discharge Simulation | |
|---------------------------|----------------------|-----------|
| | $NSE (\leq 1)$ | $r (0-1)$ |
| H1 (<i>Calibration</i>) | 0.88 | 0.94 |
| H2 (<i>Validation</i>) | 0.72 | 0.85 |
| H10 (<i>Validation</i>) | 0.73 | 0.91 |

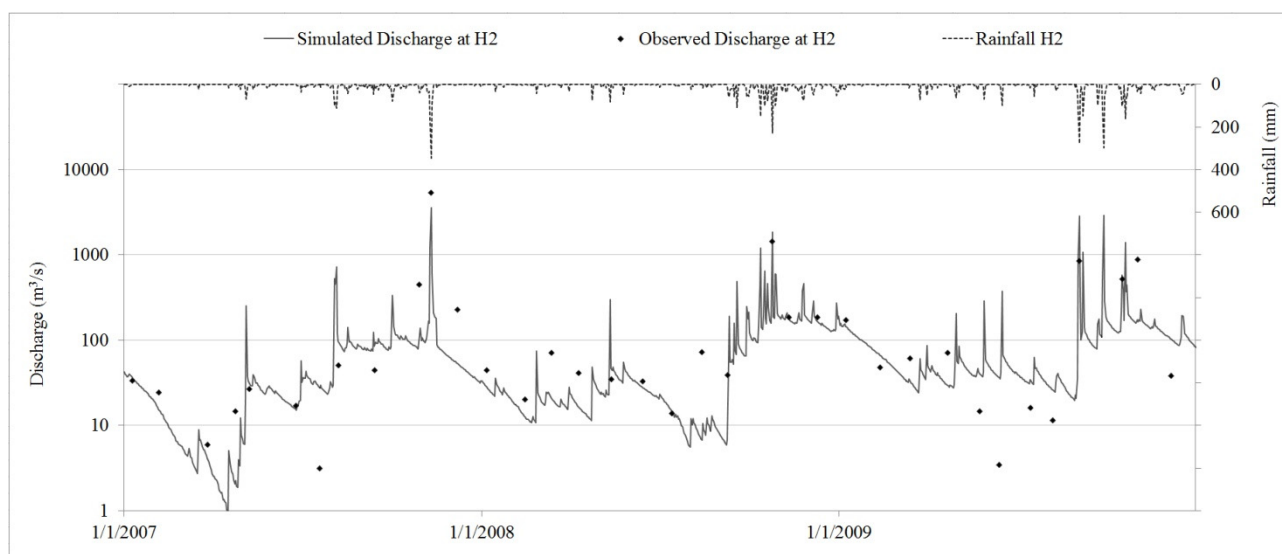


Figure 3. Discharge validation at H2.

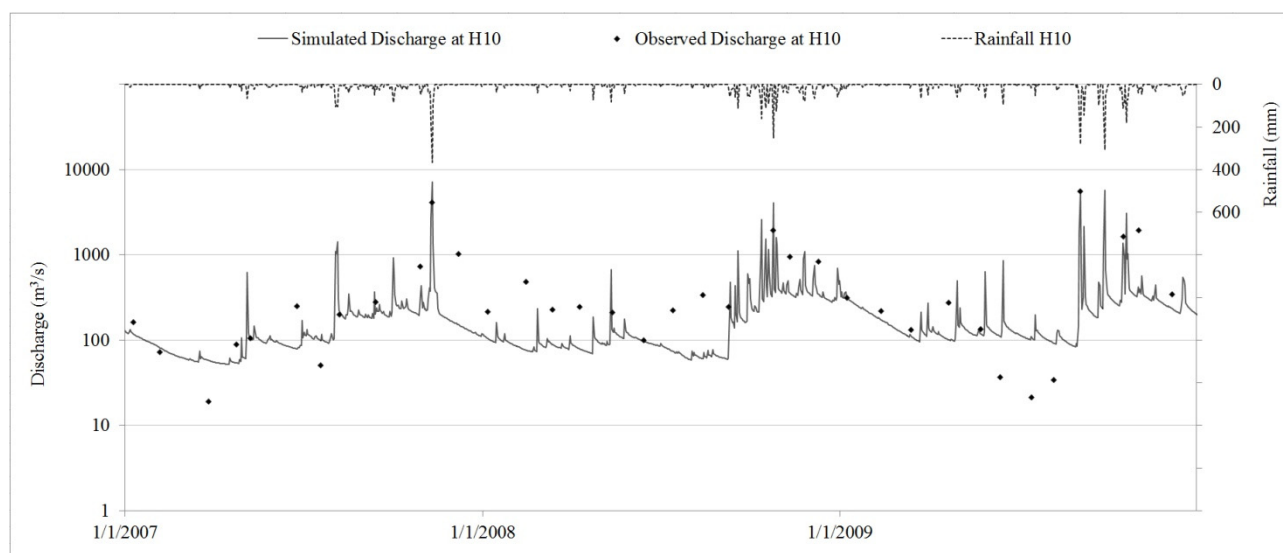


Figure 4. Discharge validation at H10.

3.2. Historical and Future Climate Data

Figure 5 illustrates the total seasonal precipitation and its standard deviation in the Huong River basin. Spatial distribution of the seasonal precipitation during the 1951–2012 period shows highest precipitation during the summer season: precipitation in excess of 1000 mm over the mountainous area of the basin with lower precipitation of about 800–950 mm in the delta area. The spatial pattern of fall precipitation is different, higher values of around 550–600 mm over the delta area with lower values of 450–500 mm in the mountain region. Precipitation in the spring is average, about 400–450 mm, and is relatively homogeneous over the basin. Winter is known as the driest season with low precipitation, below 100 mm, falling uniformly over the whole basin.

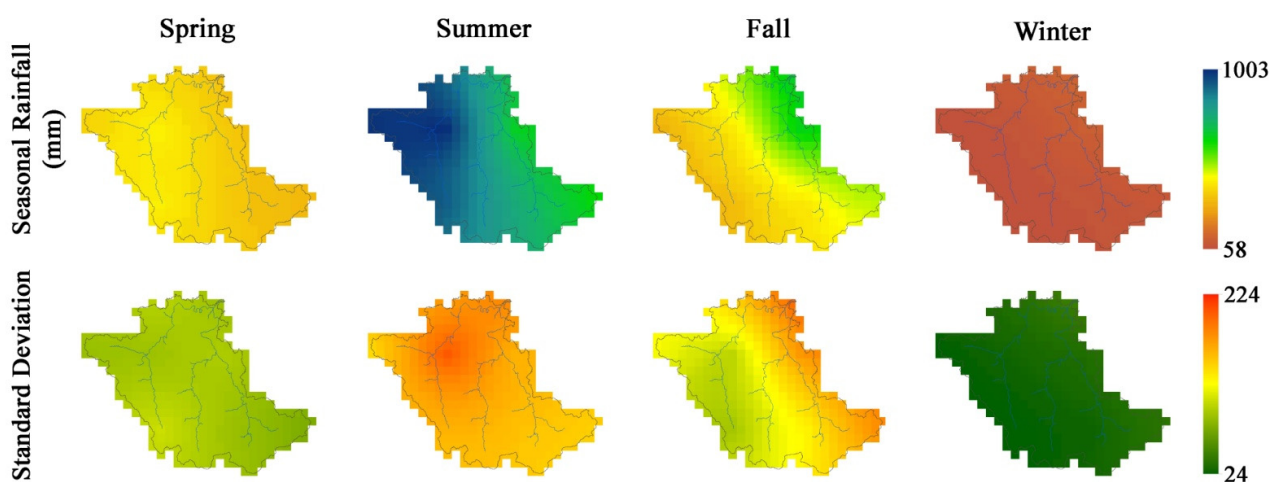


Figure 5. Seasonal precipitation distribution and their standard deviation.

Maximum daily temperature in the summer is always above 35 °C and usually around 37–39 °C; it reaches above 40 °C on rare occasions. In the winter, maximum daily temperature is usually around 13–15 °C but can reach 17–18 °C during warmer years. Summer minimum daily temperature fluctuates between 27 and 30 °C; in warmer summers the minimum daily temperature reaches above 32 °C.

The minimum daily temperature fluctuates between 12 and 13 °C in the in some years fell below 10 °C. Humidity within the Huong River basin area is always very high at 95%–100% during the rainy season. Humidity significantly decreases when temperature increases in the summer to about 45%–60%.

Historical meteorological data are input into LARS-WG to reproduce the baseline of the 1961–1990 period. Reproduced data were compared with observed data to evaluate the performance of the model. The main purpose of this step is to identify internal bias and errors of the model before simulating the future climate projections. Figure 6 illustrates the average daily precipitation graph of each month based on observed and LARS-WG-simulated values. The Nash-Sutcliffe efficiency and Pearson correlation coefficient of these two sets of data are 0.997 and 0.999 respectively; which indicates that baseline values are very well reproduced and that internal model bias and error are minimal. Calculated differences in daily precipitation are lower than 0.5 mm.

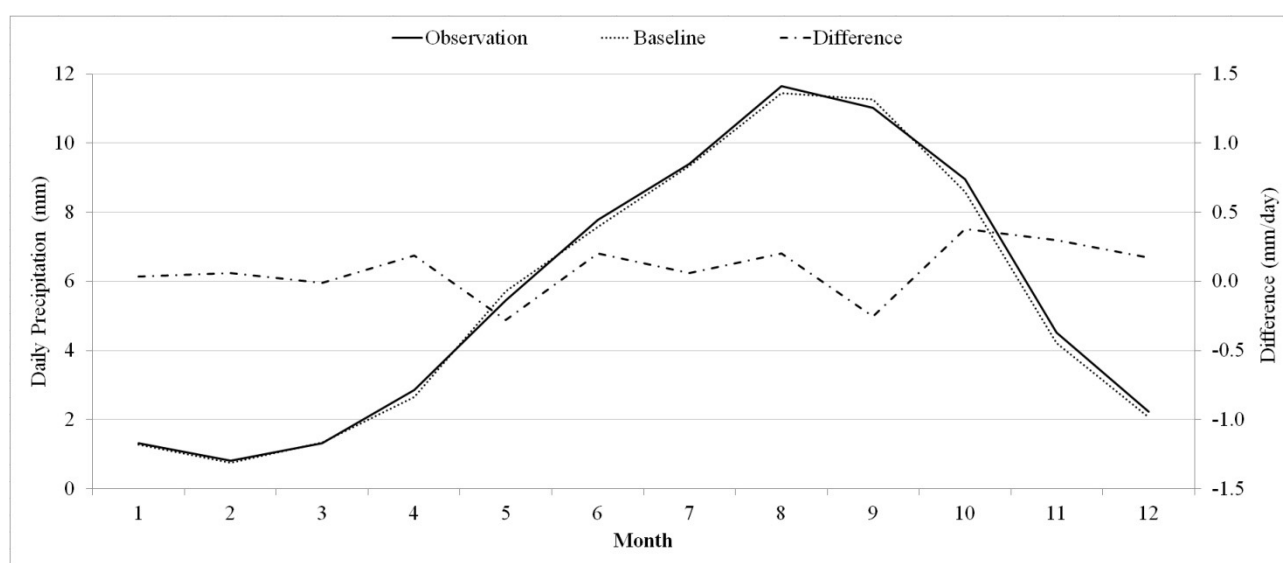


Figure 6. Average daily precipitation in 12 months from observed data (solid line–left scale) and baseline data (dotted line–left scale). The dashed line represents the differences between the two datasets (right scale).

The spatial distribution of the changes in seasonal precipitation projected by the GCMs for the 2011–2040, 2021–2050, 2031–2060, 2041–2070, 2051–2080, 2061–2090 and 2071–2100 periods are shown in Figure 7. On average, the GCMs' output data show an increase in precipitation from the present to the 2011–2040 period followed by a slight decrease until the second half of the century then a gradual increase until the end of the century. The spring season is projected to witness the most change in precipitation, a decrease of about 9% in the southern mountainous region during the 2011–2040 period. Summer and fall will stay as the wettest seasons. A considerable drop in precipitation is also projected for the winter season with the highest drop of about 8.5% in the 2071–2100 period in the south of the basin. In general, the GCMs project an increase in maximum and minimum temperature for all three IPCC-SRES scenarios in the twenty-first century. This will raise the amount of ET within the basin and reduce the total runoff that can reach the Huong River.

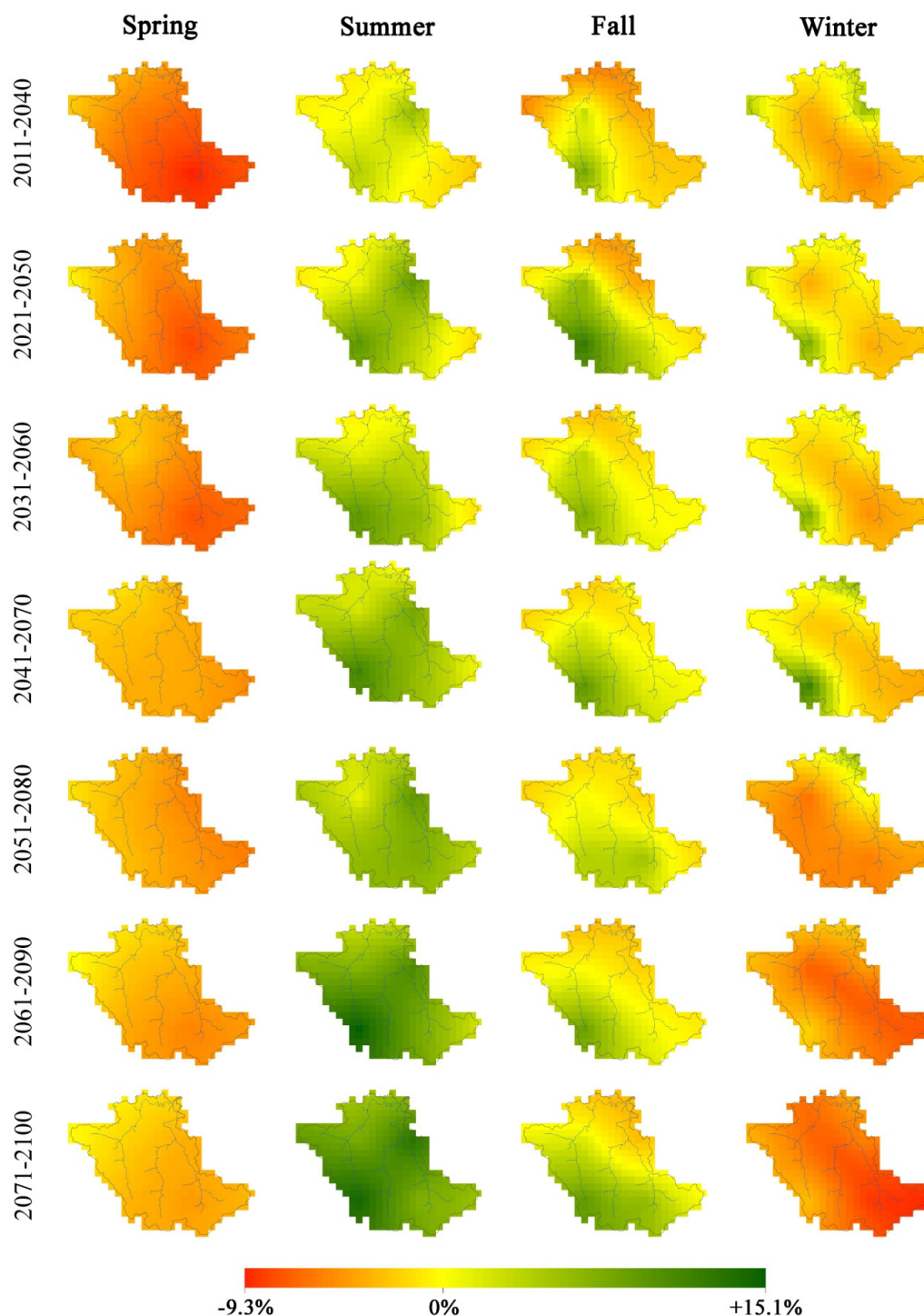


Figure 7. Change in seasonal precipitation in the 2011–2040, 2021–2050, 2031–2060, 2041–2070, 2051–2080, 2061–2090 and 2071–2100 periods compared to the baseline.

3.3. Changes in River Discharge during 1951–2012 Period

Model simulations of the Huong River discharge for the 1951–2012 period (and observations) show an increase in annual discharge. On average, the increase in annual discharge is relatively small until the end of the 20th century; however, extreme peak flows occurred more often during the last decade. Daily peak flows that exceed 2000 m³/s occurred only few times during 1951–2007 period (in 1974,

2000 and 2005); however peak flows of over 2000 m³/s have occurred in every rainy season from 2008 through 2012. Since 2000, the Huong River discharge in the rainy season increased considerably, especially from September to November, but decreased during the dry season. These changes are in response to the unusual extreme precipitation events that were observed in the first decade of the twenty-first century. Seasonal river discharge has also risen during the 1951–2012 period in general (Figure 8). Decadal average discharge indicates an increase of seasonal discharge in the fall from 1971–2000 period to 1991–2020 period. Summer discharge also increased during this period. The increase in spring and winter discharge was much more modest.

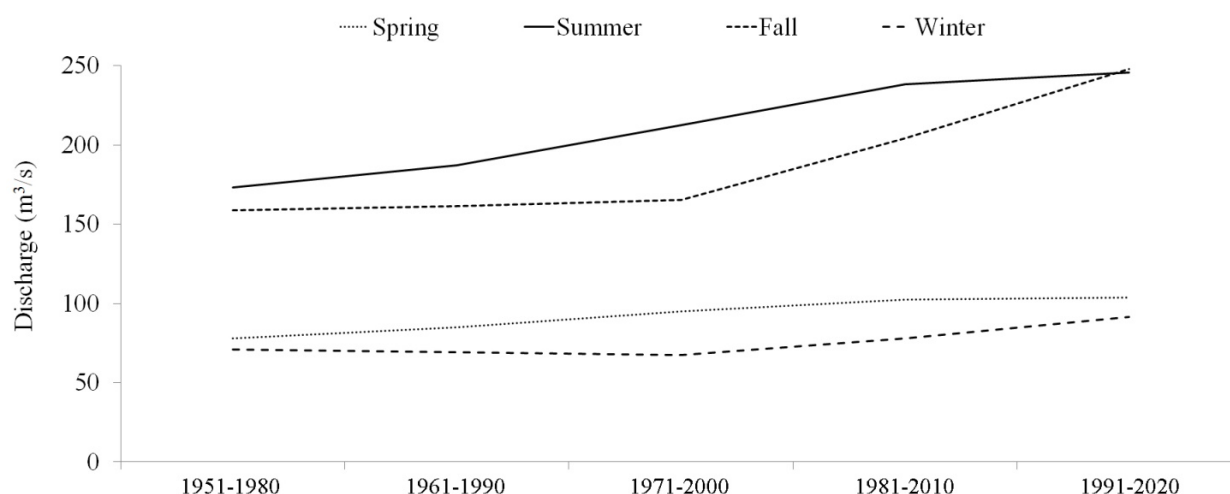


Figure 8. Average seasonal discharge from 1951 to 1980 period to 1991–2020 period.

3.4. Impact of Climate Change on River Discharge

The potential impacts of global and local climate change on water resources of the region were estimated by running the SWAT model driven by projected meteorological variables. Like other tropical rivers, the Huong River's water budget is primarily contributed mainly by direct rainfall; for that reason, any change in precipitation would alter the amount of discharge directly. Future discharge of the Huong River was simulated by forcing SWAT model with GCM outputs. Results are presented for the three preset emission scenarios for seven 30-year periods (Figure 9). Each projected discharge result is corresponding to a combination of one GCM and one emission scenario. The authors are not aware of any major land use changes in the Huong River basin and have no information on projected land use changes in the region. For these reasons, the existing land use patterns are used in the SWAT simulations. In general, the Huong River discharge is projected to continue its increase for the rest of the 21st century. Modeled ET calculations by SWAT agree with the effect of average temperature rise, especially in the winters of the 2071–2100 period and springs of the 2011–2040 period. The warming of local climate in the future that is simulated by the GCMs causes a decrease of river discharge for some periods even though precipitation is projected to increase.

In the scenario of high emission A2, there are similarities between ECHAM5-OM and HadCM3 projections. Summer is the season with the most amount of discharge, followed by fall. Spring and winter continue to have much lower discharge and river discharge is slightly higher in the spring than in the winter. The Huong River discharge is projected to increase in the summer and the fall for the rest of this

century. However, HadCM3 model projects a drop in fall discharge from the 2031–2060 period until the 2051–2080 period and then a gradual increase to the level of the 2011–2040 period. Slight decreases in seasonal discharge in the winter and the spring are also projected by ECHAM5-OM and HadCM3 models. On the contrary, GFDL-CM2.1 model projects a small decrease in discharge in the summer, especially from the 2011–2040 period to the 2051–2080 period. This model also projects winter discharge of the Huong River will increase and become higher than the spring discharge which was rarely observed in the past. The increase of fall discharge in A2 scenario is once more reinforced by GFDL-CM2.1 model.

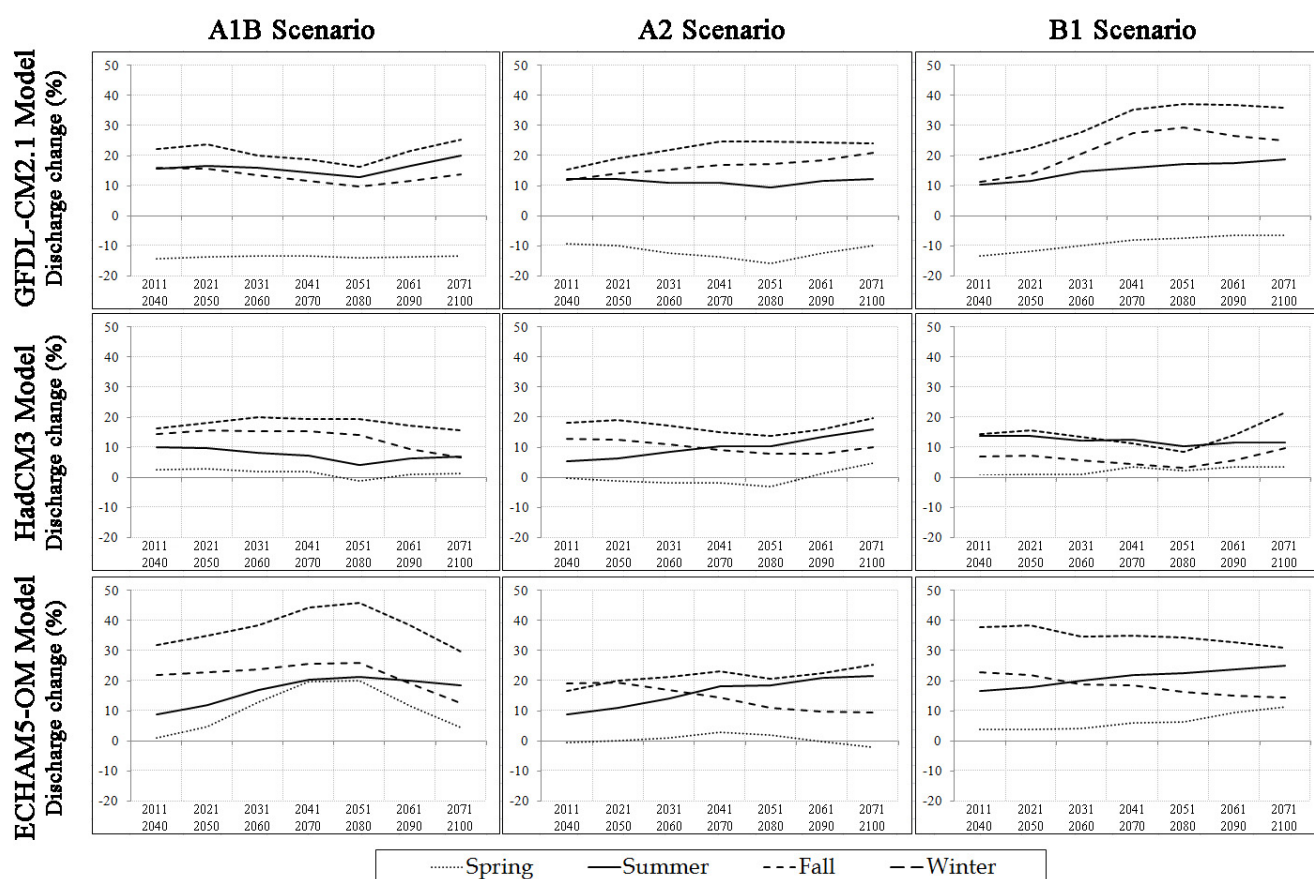


Figure 9. Projected change in total seasonal discharge in the rest of the twenty-first century produced by different GCMs in different IPCC-SRES scenarios.

Projections in the scenario of medium emission A1B show disagreements among the three climate models. Both HadCM3 and GFDL-CM2.1 models project a continuous decrease of river discharge until the 2051–2080 period and then an increase until the end of the 21st century. The ECHAM5-OM model projects that it will increase until the 2051–2080 period and then decrease for the rest of the century. HadCM3 and GFDL-CM2.1 models have similar projections for spring discharge. GFDL-CM2.1 once more projects a winter discharge that stays higher than spring discharge while HadCM3 and ECHAM5-OM models still produce normal winter discharge values that are lower than those of the spring. The Huong River discharge in the fall tends to decrease slightly in the middle of the century and increase at the end of the century as for GFDL-CM2.1 model results. HadCM3 model projects this discharge will be rather stable except a small increase in the 2051–2080 period. ECHAM5-OM model projects similar scenarios

of discharge change for the four seasons at varied levels. This model shows that in any season of the year, river discharge will keep increasing until the 2051–2080 period and then decreases until the end of the century. Seasonal discharge in the fall will sometimes become higher than summer discharge, especially in the 2011–2040, 2021–2050 and 2041–2070 periods.

Discharge projections under low emission scenario B1 also show disagreements among the three climate models, especially in the summer and the fall seasons. The GFDL-CM2.1 model projects the river discharge to increase significantly in the fall from the 2011–2040 period to the 2041–2070 period and will maintain that level to the end of the century. Summer discharge is also projected to increase in the twenty-first century. The generated winter discharge values in B1 scenario from this model are higher than the spring values and the gap between these two lines seems to widen over time. The HadCM3 model has an opposite projection that summer discharge will decrease through the twenty-first century and fall discharge will decrease similarly just until the 2051–2080 period and will climb up afterwards. Both HadCM3 and ECHAM5-OM models project minimal change in winter and spring discharge within the whole twenty-first century. However, ECHAM5-OM model projects summer discharge to increase and fall discharge to decrease.

The disagreement among three GCMs' projections is caused by different numerical equations used in the GCMs. However, all three GCMs agree that the Huong River discharge in the spring will not change significantly in the twenty-first century under any emission scenario. Winter discharge is also projected to undergo quantitatively insignificant changes, except the divergence between GFDL-CM2.1 model and the other two models due to model performance. Summer and fall discharge will vary with different possibilities of increasing and decreasing and those variations are significant. Figure 10 provides details on annual projection of seasonal discharge of the Huong River. Previous studies generated projections for South East Asia indicate an increase in runoff from 10%–20% to 40%–50% in the 21st century depending on different GCMs and emission scenarios (e.g., [13,19]). This also agrees with the projections that we obtained in this study.

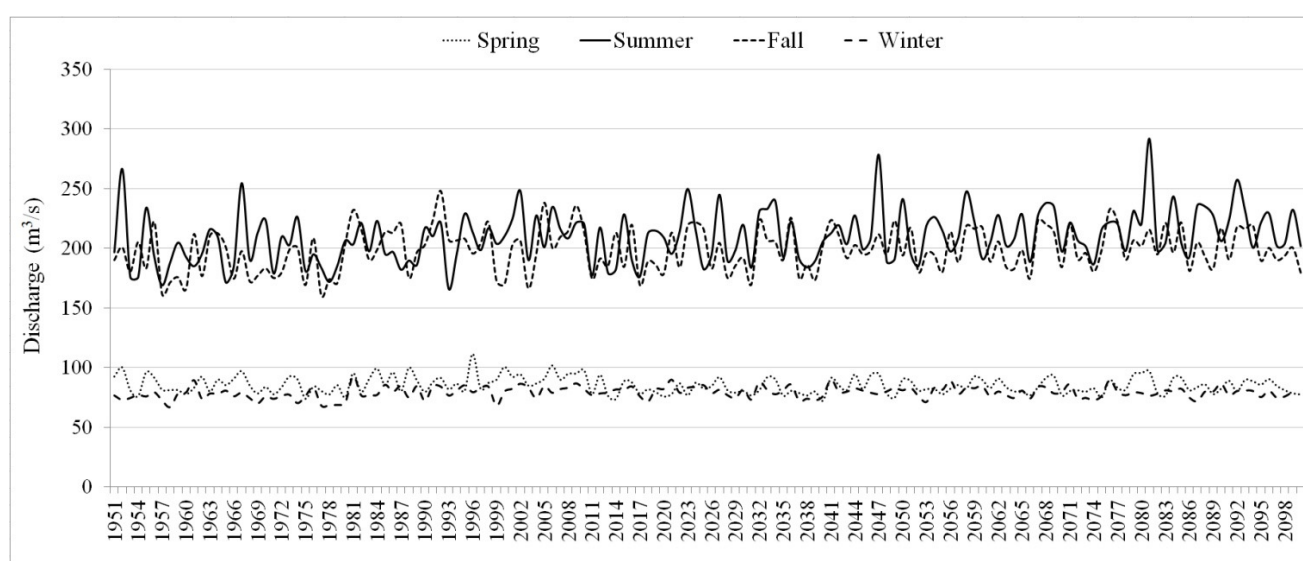


Figure 10. Historical and projected seasonal discharge from 1951 to 2100 (average of all GCMs and IPCC-SRES scenarios).

4. Summary and Conclusions

This paper used the stochastic weather generator LARS-WG and the hydrologic model SWAT to study projected future water availability in the Huong River basin in Central Vietnam. Future meteorological parameters are projected by three popular GCMs, ECHAM5-OM, HadCM3 and GFDL-CM2.1, for three IPCC-SRES scenarios A2, A1B and B1. Future projections of climate and discharge data were compared to baseline period from 1951 to 2012. The main source of the precipitation data for the baseline period was the gage-based APHRODITE precipitation product, which is complemented by observation in the later years. Other historical meteorological data were based on *in-situ* measurements and satellite observations. LARS-WG and SWAT were first calibrated and validated over the study area. LARS-WG was used to simulate meteorological conditions during the historical period and its results compared very well against observations. SWAT model was also calibrated and validated over the Huong River basin against monthly observed discharge data. Results of SWAT model calibration and validation were adequate with a Nash-Sutcliffe efficiency coefficient of 0.88 and a correlation coefficient of 0.94.

Over the historical period, the Huong River discharge has been increasing since the 1951–1980 period. In particular, the fall discharge has increased significantly since the 1971–2000 period while the summer discharge has increased most between the 1970's and 1981–2010 period. According to models' projections for seasonal Huong River discharge in the twenty-first century, this increase in the summer and fall will continue with A2 and B1 emission scenarios modeled by the three GCMs. Changes in winter and spring discharge appear insignificant. In most of the cases, it is projected to slightly decrease during the 21st century. However, detailed analyses indicate differences in possible changes of seasonal river discharge in the future among different GCMs and climate scenarios. Although precipitation is the most important agent in changing in discharge, the projection of the Huong River discharge is not always proportional to the projected change in precipitation under the same IPCC-SRES scenario and using the same GCM. An obvious explanation is that ET will rise significantly due to the increase of temperature and that reduces the total amount of runoff.

The intent of this paper is to generate data that may aid decision makers in making decisions that will ensure sustainability of water resources in the region. The Huong River is witnessing intense on-going water resources management activities, the details of which are not completely available to the authors, e.g., dam construction and operation policies. Thus, simulations of future discharge do not include the impacts of management and flow regulation. Nonetheless, the study presents results that may help guide water resources planning and management in the region by quantitatively providing potential changes in river flow in the 21st century.

Acknowledgments

Support of the Environmental Science and Engineering program, University of Texas at San Antonio to the first author is cordially acknowledged.

Author Contributions

This paper presents part of Tuan Le study research. Tuan Le's study was advised by Hatim O. Sharif who guided his research and contributed significantly to preparing the manuscript for publication.

Conflicts of Interest

The authors declare no conflicts of interest.

References

1. Arnell, N.W. Climate change and global water resources. *Glob. Environ. Chang.* **1999**, *9*, 831–849.
2. Arnell, N.W. Effects of IPCC SRES emissions scenarios on river runoff: A global perspective. *Hydrol. Earth Syst. Sci.* **2003**, *7*, 619–641.
3. Arnell, N.W. Climate change and global water resources: SRES emissions and socioeconomic scenarios. *Glob. Environ. Chang.* **2004**, *14*, 31–52.
4. Vorosmarty, C.J.; Green, P.; Salisbury, J.; Lammers, R.B. Global water resources: Vulnerability from climate change and population growth. *Science* **2000**, *289*, 284–288.
5. Oki, T.; Kanae, S. Global hydrological cycles and world water resources. *Science* **2006**, *313*, 1068–1072.
6. Intergovernmental Panel on Climate Change (IPCC). *Climate Change 2013: The Physical Science Basis. Contribution of Working Group I to the Fifth Assessment Report of the Intergovernmental Panel on Climate Change*; Cambridge University Press: Cambridge, UK, 2013.
7. Felzer, B.; Heard, P. Precipitation Differences amongst GCMs Used for the U.S. National Assessment. *J. Am. Water Resour. Assoc.* **1999**, *35*, 1327–1340.
8. Nijseen, B.; O'Donnell, G.M.; Hamlet, A.F.; Lettenmaier, D.P. Hydrologic sensitivity of global rivers to climate change. *Clim. Chang.* **2001**, *50*, 143–175.
9. Arreguin-Cortes, F.I.; Lopez-Perez, M. Impacts of climate change on the hydrological cycle in Mexico. *Int. J. Water Resour. Dev.* **2013**, *29*, 172–183.
10. Rasilla, D.F.; Garmendia, C.; Carlos, J. Climate change projections of streamflow in the Iberian Peninsula. *Int. J. Water Resour. Dev.* **2013**, *29*, 184–200.
11. Hashmi, M.Z.; Shamseldin, A.Y.; Melville, B.W. Comparison of SDSM and LARS-WG for simulation and downscaling of extreme precipitation events in a watershed. *Stoch. Environ. Res. Risk Assess.* **2011**, *25*, 475–484.
12. Sanderson, M.G.; Wiltshire, A.J.; Betts, R.A. Projected changes in water availability in the United Kingdom. *Water Resour. Res.* **2012**, *48*, W08512.
13. Weiland, F.C.S.; van Beek, L.P.H.; Kwadijk, J.C.J.; Bierkens, M.F.P. Global patterns of change in discharge regimes for 2100. *Hydrol. Earth Syst. Sci.* **2012**, *16*, 1047–1062.
14. Wu, H.; Kimball, J.S.; Elsner, M.M.; Mantua, N.; Adler, R.F.; Stanford, J. Projected climate change impacts on the hydrology and temperature of Pacific Northwest rivers. *Water Resour. Res.* **2012**, *48*, W11530.
15. Hamlet, A.F. Assessing water resources adaptive capacity to climate change impacts in the Pacific Northwest Region of North America. *Hydrol. Earth Syst. Sci.* **2011**, *15*, 1427–1443.

16. Thodsen, H. The influence of climate change on stream flow in Danish rivers. *J. Hydrol.* **2007**, *333*, 226–238.
17. Institute of Strategy and Policy On Natural Resources and Environment of Vietnam (ISPONRE). *Vietnam Assessment Report on Climate Change*; Vanhoa-Thongtin Publishing House: Hanoi, Vietnam, 2009.
18. Milly, P.C.D.; Dunne, K.A.; Vecchia, A.V. Global pattern of trends in streamflow and water availability in a changing climate. *Nature* **2005**, *438*, 347–350.
19. Nohara, D.; Kitoh, A.; Hosaka, M.; Oki, T. Impact of climate change on river discharge projected by multimodel ensemble. *J. Hydrometeorol.* **2006**, *7*, 1076–1089.
20. Chen, T.C.; Tsay, J.D.; Yen, M.C.; Matsumoto, J. Interannual variation of the late rainfall in central Vietnam. *J. Clim.* **2012**, *25*, 392–413.
21. Yen, M.C.; Chen, T.C.; Hu, H.L.; Tzeng, R.Y.; Dinh, D.T.; Nguyen, T.T.T.; Wong, C.J. Interannual variation of the Fall rainfall in Central Vietnam. *J. Meteorol. Soc. Jpn.* **2011**, *89A*, 259–270.
22. Prime Minister of Vietnam (PM-Vietnam). *Decision No 1570/QD-TTg: Approved Strategy for Sustainably Exploitation and Usage of Natural Resources and Marine Environment Protection until 2020, Vision to 2030*; PM-Vietnam: Hanoi, Vietnam, 2013.
23. Ngo, D.T. *Effective Usage and Development of Water Resources*; Biodiversity and Climate Change Conference: Connection to Poverty and Sustainable Development: Hanoi, Vietnam, 2007.
24. Applications of the MIKE 11 Model for Evaluating the Effectiveness in Flood Control of the Reservoirs in Upstream of the Huong River. Available online: http://lib.wru.edu.vn/index.php?option=com_content&view=category&layout=blog&id=15&Itemid=196&limitstart=8 (accessed on 3 February 2014).
25. Hydropower Development on Huong River Basin, Limitations and the Measures to Improve the Benefits. Available online: http://lib.wru.edu.vn/index.php?option=com_content&view=category&layout=blog&id=15&Itemid=196&limitstart=5 (accessed on 3 February 2014).
26. Nguyen, T.; Nguyen, H.S. Impact of climate change in the watershed of Huong River, Thua Thien Hue Province. *J. Sci. Hue Univ.* **2010**, *58*, 107–119.
27. Intergovernmental Panel on Climate Change (IPCC). *Climate Change 2007: The Physical Science Basis. Contribution of Working Group I to the Fourth Assessment Report of the Intergovernmental Panel on Climate Change*; Cambridge University Press: Cambridge, UK, 2007.
28. Le, T.B.; Al-Juaidi, F.H.; Sharif, H. Hydrologic Simulations Driven by Satellite Rainfall to Study the Hydroelectric Development Impacts on River Flow. *Water* **2014**, *6*, 3631–3651.
29. Semenov, M.A.; Stratonovitch, P. Use of multi-model ensembles from global climate models for assessment of climate change impacts. *Clim. Res.* **2010**, *41*, 1–14.
30. Semenov, M.A.; Brooks, R.J.; Barrow, E.M.; Richardson, C.W. Comparison of the WGEN and LARS-WG stochastic weather generators for diverse climates. *Clim. Res.* **1998**, *10*, 95–107.
31. Racsco, P.; Szeidl, L.; Semenov, M.A. A serial approach to local stochastic weather models. *Ecol. Model.* **1991**, *57*, 27–41.
32. LARS-WG Stochastic Weather Generator. Available online: <http://www.rothamsted.ac.uk/mas-models/larswg.php> (accessed on 1 June 2015).

33. Covey, C.; AchutaRao, K.M.; Cubasch, U.; Jones, P.; Lambert, S.J.; Mann, M.E.; Phillips, T.J.; Taylor, K.E. An overview of results from the Coupled Model Intercomparison Project. *Glob. Planet. Chang.* **2003**, *37*, 103–133.
34. Institute of Resources, Environment, and Biotechnology of Hue University, Vietnam (IREB-Hue). *Annual Reports on Water Quality Monitoring Results of Huong River*; IREB-Hue: Hue, Vietnam, 2003–2010.
35. Veith, T.L.; van Liew, M.W.; Bosch, D.D.; Arnold, J.G. Parameter sensitivity and uncertainty in SWAT: A comparison across five USDA-ARS watersheds. *Am. Soc. Agric. Biol. Eng.* **2009**, *53*, 1477–1486.
36. Santhi, C.; Arnold, J.G.; Williams, J.R.; Dugas, W.A.; Srinivasan, R.; Hauck, L.M. Validation of the SWAT model on a large river basin with point and nonpoint sources. *J. Am. Water Resour. Assoc.* **2001**, *37*, 1169–1188.
37. Van Liew, M.W.; Garbrecht, J. Hydrologic simulation of the Little Washita River experimental watershed using SWAT. *J. Am. Water Resour. Assoc.* **2003**, *39*, 413–426.
38. Moriasi, D.N.; Arnold, J.G.; van Liew, M.W.; Bingner, R.L.; Harmel, R.D.; Veith, T.L. Model evaluation guidelines for systematic quantification of accuracy in watershed simulations. *Trans. ASABE* **2007**, *50*, 885–900.
39. Yatagai, A.; Krishnamurti, T.N.; Humar, V.; Mishra, A.K.; Simon, A. Use of APHRODITE rain gauge-based precipitation and TRMM 3B43 products for improving Asian monsoon seasonal precipitation forecasts by the superensemble method. *J. Clim.* **2014**, *27*, 1062–1069.